African Journal of Pharmacy and Pharmacology Vol. 6(30), pp. 2322-2331, 15 August, 2012
Available online http://www.academicjournals.org/AJPP
DOI: 10.5897/AJPP12.1048
ISSN 1996-0816 ©2012 Academic Journals

Full Length Research Paper

Ab initio studies of single-wall carbon nanotube for drug delivery of (N-acetyl-L-cysteinato-O, S) diphenyl tin (IV) anticancer drug

Amir Sobhanmanesh[1]*, Majid Monajjemi[1], Karim Zare[1] and Golnaz shams[2]

[1]Department of Chemistry, Science and Research Branch, Islamic Azad University, Tehran, Iran.
[2]Department of Entomology, Science and Research Branch, Islamic Azad University, Tehran, Iran.

Accepted 23 April, 2012

Carbon nanotubes (CNT) have emerged as a new alternative and efficient tool for transporting and translocating therapeutic molecules. CNT can be attached to drugs, and used to deliver their cargos to cells and organs. In this work, the interaction behavior of the anticancer drug $Sn(C_6H_5)_2$(N-acetyl-L-cysteinate) that is called (N-acetyl-Lcysteinato-O,S) diphenyl tin (IV) when binding single-walled carbon nanotubes was studied based on the Quantum chemical *ab initio* calculations by using the HF/ (LanL2DZ+STO-3G) and HF/ (LanL2DZ+6-31G) levels in both gas phase and solution. Thermodynamical analysis (large negative values of the ΔG and high positive values of ΔS) confirmed the structural stability of the $Sn(C_6H_5)_2$(N-acetyl-L-cysteinato-O,S) – CNT in both gas phase and in solution. Also, The thermodynamic analysis show that $Sn(C_6H_5)_2$(N-acetyl-L-cysteinato-O,S) – CNT has maximum stability in methanol at 313K. Moreover, nuclear magnetic resonance (NMR) parameters such as chemical shift tensor (δ), total atomic charge and asymmetry parameter (η) have been calculated using the Gauge Independent Atomic Orbital (GIAO) method, results being compared with CGST data. From the NMR calculations, it can be seen that the NMR parameters (δ, η) at the sites of nitrogen and oxygen are significantly influenced by intermolecular hydrogen- bonding interactions but the quantity at the site of S-27 is influenced by nonspecific solute-solvent interaction such as polarisability/polarity.

Key words: $Sn(C_6H_5)_2$(N-acetyl-L-cysteinate), *ab initio*, single wall carbon nanotubes (SWCNT), drug delivery.

INTRODUCTION

The chemistry of organotin (IV) has witnessed an increased interest during the last fifty years, owing to their potential biological and industrial applications. However, some organotin (IV) compounds, which were originally modeled on the first tumor-active platinum compound, cisplatin (Barnard, 1989), have also found their place among a class of non-platinum chemotherapeutic metallopharmaceuticals exhibiting good antitumor activity (Clarke et al., 1999; Nath et al., 2001). In this context, Diorganotin (IV) derivatives and mainly those of dialkyltin (IV) complexes from amino acids ligand are known to possess antimicrobial (Plesch et al., 1988), antimalarial (Goldberg et al., 1997), antiproliferative (K♀pf-Maier and K♀pf, 1987), chemotherapeutic (Wang et al., 2005), radiopharmaceutical (Wang and Meng, 2006), insulin-mimetic (Pessoa et al., 1999) and fungicidal (Eng et al., 1996) activities. Further, tin (IV) complexes characterized by the presence of amino acid ligands have proved to be cytotoxic against the breast adenocarcinoma tumor MCF-7, the colon carcinoma (Gielen, 1996) and hepatocarcinoma HCC Hep G2 cancer, (Pellerito et al., 2010). In 2010 Girasolo et al. reported the antitumor activity of organotin(IV) complexes containing L-Arginine, Nα-t-Boc-L-Arginine and L-Alanyl-L-Arginine against the Human colon-rectal carcinoma HT29, observing that for all these complexes, cytotoxic activity was higher than that exerted by cisplatin (Girasolo et al., 2010).

In 2010 Tzimopoulos et al. reported the results of a screening on wide range of triorganotin aminobenzoates in the K562 myelogenous leukaemia, HeLa

*Corresponding author. E-mail: amirsobhanmanesh@yahoo.com. Tel: +989179113508. Fax: +982144865464.

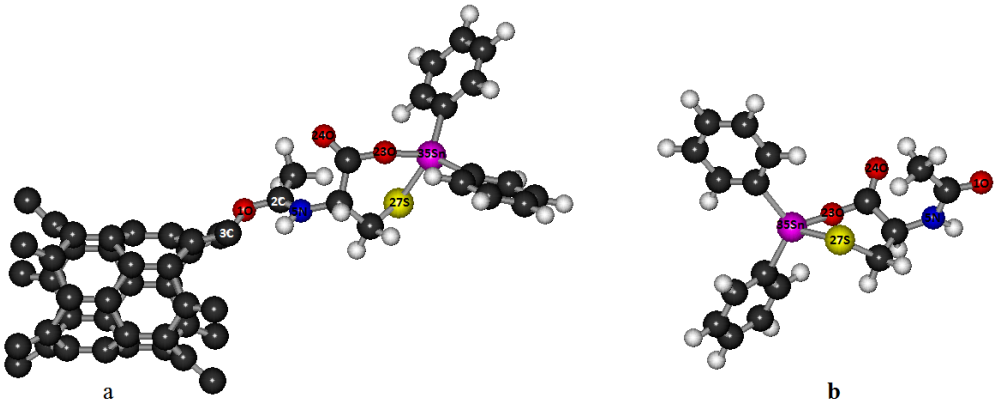

Figure 1. Optimized geometry of the $Sn(C_6H_5)_2$(N-acetyl-L-cysteinato-O,S) – CNT complex (a) and $Sn(C_6H_5)_2$(N-acetyl-L-cysteinato-O,S) (b), obtained at the (LanL2DZ+6-31G) level.

cervical cancer and HepG2 hepatocellular carcinoma cells, observing that for triorganotin complexes containing aminobenzoates, cytotoxic activity was better than cisplatin and some triorganotin carboxylates drugs (Tzimopoulos et al., 2010). Furthermore, the cytotoxic activity of Diorganotin (IV) N-acetyl-L-cysteinate complexes towards Human hepatocarcinoma HCC Hep G2 cells were studied by Lorenzo Pellerito and Cristina Prinzivalli in 2010. As result Sn(C6H3)2(N-acetyl-L-cysteine) has been proposed as a therapeutic against the human hepatocarcinoma HCC Hep G2 cells (Pellerito et al., 2010). In the case at hand, since the discovery of carbon nanotubes (CNTs) (Iijima, 1991), they have been considered as the ideal material for a variety of applications owing to their unique properties. These properties include their potential biocompatibility in pharmaceutical drug delivery systems and their excellent role as drug carriers with a highly site-selective delivery and sensitivity (Bianco et al., 2005; Mollaamin et al., 2010a; Popov et al., 2007; Banerjee et al., 2005; Pastorin et al., 2006; Klumpp et al., 2006; Kostarelos et al., 2007; Raffa et al., 2008; Zhang et al., 2009; Monajjemi et al., 2010b).

To accelerate the optimal development of CNT as a new effective drug transporter, it is required to better understand the structural properties of the drug–CNT complex. In this paper we reported a computational study of the interaction between Diorganotin (IV) complexes of N-acetyl-L-cysteine (H2NAC; (R)-2-acetamido-3-sulfanylpropanoic acid) whit CNT. We perform a full geometrical, energetical, nuclear magnetic resonase, and vibrational analysis of $Sn(C_6H_5)_2$(N-acetyl-L-cysteinato-O,S) – CNT with different basis set to elucidate the effect of site-specific of these systems. The aim of this study was to investigate the stability of $Sn(C_6H_5)_2$(N-acetyl-L-cysteinato-O,S) – CNT at physiological conditions (temperature, solvent, etc.) and examine the effect of dielectric constant on stability of $Sn(C_6H_5)_2$(N-acetyl-L-cysteinato-O,S) – CNT complex.

COMPUTATIONAL METHODS

The armchair carbon nanotube (5,5) that simulated in this study containing 60 carbon atoms, with both ends opened. In our model, $Sn(C_6H_5)_2$(NCA)was attached covalently to carbon nanotube (CNT). All calculations for $Sn(C_6H_5)_2$(N-acetyl-L-cysteinato-O,S) – CNT were carried out by employing the GAUSSIAN 98 suite of programs (Frisch et al., 1998). Full geometry optimization and further frequency analysis were performed using Hartree-Fock (HF) level of theory in conjunction with the LanL2DZ basis set for Sn atom only (Mollaamin et al., 2010b; Monajjemi et al., 2010a; Hay and Wadt, 1985; Wadt and Hay, 1985) and STO-3G and 6-31G basis sets for other atoms. This was done for calculating the Gibbs free energy (ΔG) as well as entropy changes (ΔS) in both gas phase and in solution. The NMR parameters (such as Chemical shifts (δ), asymmetry parameter (η) and total atomic charges) were also evaluated on the optimized geometries employing the Gauge Independent Atomic Orbital (GIAO) and Continuous set of gauge transformations (CSGT) methods (Wrackmeyer 1985; Ditchfield 1972; Pulay et al., 1990; Keith and Bader, 1993). Moreover, the solvent effect is taken into account via the self-consistent reaction field (SCRF) approach (Miertus et al., 1981; Miertus and Tomasi, 1982; Monajjemi and Chahkandi, 2005).

RESULTS AND DISCUSSION

Molecular geometry

Figure 1 denotes the optimized structures of the $Sn(C_6H_5)_2$(N-acetyl-L-cysteinato-O,S) and $Sn(C_6H_5)_2$(N-acetyl-L-cysteinato-O,S) – CNT whit active sites labeling. Also, some of selected parameters for the $Sn(C_6H_5)_2$(N-acetyl-L-cysteinato-O,S) – CNT such as relative energy (kcal/mol) and dipole moments (Debye) are listed in

Table 1. Calculated relative energy (kcal/mol) and dipole moments (μ in Debye) of the $Sn(C_6H_5)_2$(N-acetyl-L-cysteinato-O,S) – CNT complex obtained at the (LanL2DZ+STO-3G) and (LanL2DZ+6-31G) levels.

Phase/solvent	E (RHF)		E (Kcal/mol)		Dipole moment (Debye)	
Basis set	HF/Sto-3G	HF/6-31G	HF/Sto-3G	HF/6-31G	HF/Sto-3G	HF/6-31G
Gas phase	-2811.97925162	-2845.69296503	-1764520.9452822947842	-1785676.3479834056923	9.4891	23.2198
In water	-2811.98223377	-2845.71912981	-1764522.8165856246157	-1785692.7664197480321	11.3497	41.1363
In methanol	-2811.98211572	-2845.71790385	-1764522.7425090831652	-1785691.9971281194285	11.1915	40.2412
In ethanol	-2811.98205148	-2845.71724484	-1764522.7021983925868	-1785691.5835984152244	11.1059	39.7634

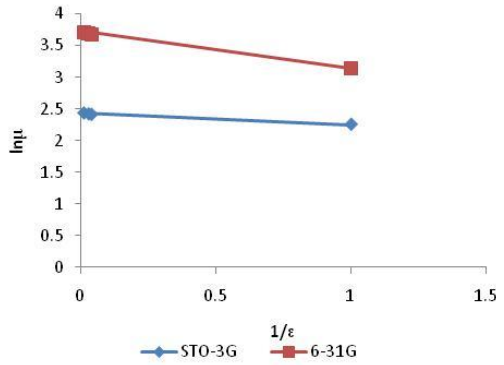

Figure 2. Plot of the lnμ (Debye) versus the 1/ε, obtain from the (LanL2DZ+STO-3G) and (LanL2DZ+6-31G) calculations for $Sn(C_6H_5)_2$(N-acetyl-L-cysteinato-O,S) – CNT Complex.

Table 1. The results show that the calculated energy and dipole moment of $Sn(C_6H_5)_2$(N-acetyl-L-cysteinato-O,S) – CNT are increased by increasing dielectric constant (ε) of solvent. The double reciprocal plot of lnμ versus 1/ε in gas phase and various solvents are shown in Figure 2.

Calculated NMR parameters

The calculated NMR parameters (such as Chemical shift (δ), asymmetry parameter (η) and total atomic charges) for active sites of $Sn(C_6H_5)_2$(N-acetyl-L-cysteinato-O,S) – CNT, are given in Table 2. Also, the graphs of calculated Chemical shifts (δ), asymmetry parameter (η) and total atomic charges versus the number of atomic centers for selected atoms of $Sn(C_6H_5)_2$(N-acetyl-L-cysteinato-O,S) – CNT system are displayed in Figures 3a to c respectively. As shown in Figure 3c, the Sn-35 nucleus has maximum total atomic charge and low δ values in both gas phase and in solution, meaning the relative chemical shift at the site of Sn-35 is predominantly governed by local diamagnetic shielding term (σ^d). Further, Tin atom has large amounts of asymmetry parameter (η) in both gas phase and in solution (sees Figure 3b). The results show that the calculated chemical shift tensor and asymmetry parameter at the site of Sn-35 are reduced by increasing dielectric constant (ε) of solvent (Figure 3a). The observed changes can be due to presence of the solvent molecule in the Tin inner coordination sphere. Since S-27 is more negative than Sn-35 (Figure 3c), this difference in the charges leads to a smaller chemical shift tensor (δ) for the sulfur atom (Figure 3a). The results in Figure 3a show that, with increase of dielectric constant from gas phase to water, the δ values at the site of sulfur atom increases. The observed effect is probably due to the nonspecific solute-solvent interaction (such as polarisability/polarity) at the site of S-27 nucleus. Since N has a lone pair of electrons in the valance shell, the electronic environment at the site of N is completely different from that of Sn, therefore, different behaviors are expected. This leads to the lower chemical shift values for the nitrogen atom (Figure 3a). The results in solution indicate that, the chemical shift tensor (δ) at the site of N-5 decreases in the order Gas Phase > Water > Ethanol > Methanol. In this regard, it seems that the chemical shift tensor at the site of N-5 nucleus is significantly influenced by intermolecular hydrogen- bonding interactions. Since carbon atoms (C-2 and C-3) are more positive than N-5 (Figure 3c), the δ values at the sites of C-2 and C-3 are greater than the N-5 nucleus (Figure 3a). The results show that the calculated chemical shift tensor and asymmetry parameter at the site of C-2 are reduced by increasing dielectric constant (ε) of solvent (Figure 3a and b). Furthermore, the calculated chemical shift tensor at the site of C-3 is reduced by increasing dielectric constant (ε) of solvent (Figure 3a). As shown in Figure 3b, C-3 has maximum asymmetry parameter in both water and Methanol, but the quantity in gas phase is minimum. Moreover, the chemical shift constants for the C-3 are larger than chemical shifts values for the C-2. This observation indicates that the C-2 is more shielded than the C-3 nucleus. It should be noted that C-2 nucleus has the greater η

Table 2. Calculated NMR parameters of $Sn(C_6H_5)_2$(N-acetyl-L-cysteinato-O,S) – CNT complex in gas phase and various solvents at GIAO and CSGT method.

Atoms	Δ				H				Charge			
	GIAO		CSGT		GIAO		CSGT		GIAO		CSGT	
	HF/STO-3G	HF/6-31G	HF/STO-3G	HF/6-31G	HF/STO-3G	HF/6-31G	HF/STO-3G	HF/6-31G	HF/STO-3G	HF/6-31G	HF/STO-3G	HF/6-31G
						Gas phase						
1O	149.0242	270.3139	130.8648	257.8294	0.138392	0.087549	0.72994	0.065623	-0.19367	-0.76844	-0.19367	-0.76844
5N	137.0314	-140.103	-123.962	-140.451	0.767358	0.752471	0.576403	0.395483	-0.3738	-0.96905	-0.3738	-0.96905
23O	593.6829	506.8701	457.5637	438.5751	0.442454	0.378132	0.264253	0.424838	-0.23417	-0.5324	-0.23417	-0.5324
24O	37.5792	-126.16	-34.3105	-145.771	0.769042	0.626849	0.138742	0.517359	-0.33101	-0.90003	-0.33101	-0.90003
27S	203.8254	139.4606	-151.63	-139.746	0.280375	0.88155	0.818837	0.824889	0.049421	-0.27264	0.049421	-0.27264
35Sn	-4.5841	-3.3452	-4.5042	3.2571	0.522633	0.985801	0.78953	0.895981	0.526593	1.783351	0.526593	1.783351
2C	-47.177	121.4287	-32.0628	123.4359	0.289531	0.569121	0.46796	0.471298	0.245502	0.927947	0.245502	0.927947
3C	86.4499	-274.304	75.3443	-267.147	0.193959	0.024732	0.496049	0.087031	0.079401	0.24033	0.079401	0.24033
						Water						
1O	151.7131	272.34	132.8003	261.849	0.126644	0.193906	0.753713	0.079657	-0.19389	-0.76788	-0.19389	-0.76788
5N	136.1049	-142.382	-123.797	-141.149	0.746149	0.872626	0.567151	0.506131	-0.37362	-0.96513	-0.37362	-0.96513
23O	592.2061	496.0106	456.837	426.8305	0.443363	0.398766	0.264554	0.471952	-0.23424	-0.54585	-0.23424	-0.54585
24O	37.5217	-127.113	-34.9522	-147.984	0.75209	0.691053	0.13471	0.538829	-0.33389	-0.87797	-0.33389	-0.87797
27S	202.2831	-123.306	-151.151	-135.515	0.295098	0.999492	0.813059	0.696511	0.048433	-0.27743	0.048433	-0.27743
35Sn	-4.551	-3.5516	-4.4467	3.2057	0.527466	0.864371	0.762251	0.933774	0.527578	1.794255	0.527578	1.794255
2C	-48.4571	118.7468	-33.0871	121.2403	0.243265	0.703378	0.390291	0.631234	0.249783	0.926535	0.249783	0.926535
3C	85.7514	-342.939	75.2883	-330.226	0.221726	0.124264	0.512995	0.06738	0.079324	0.282279	0.079324	0.282279
						Methanol						
1O	151.9503	271.7766	132.9426	261.289	0.124139	0.181824	0.756078	0.065711	-0.194	-0.76811	-0.194	-0.76811
5N	136.1414	-142.284	-123.775	-141.119	0.746452	0.86511	0.570508	0.499591	-0.37363	-0.96561	-0.37363	-0.96561
23O	593.0419	496.2566	457.5026	427.1057	0.442207	0.397422	0.263622	0.469237	-0.23429	-0.54484	-0.23429	-0.54484
24O	37.4594	-127.329	-34.9035	-148.112	0.753095	0.68847	0.135571	0.538483	-0.33344	-0.87901	-0.33344	-0.87901
27S	202.4667	124.2449	-150.969	-135.884	0.295853	0.993235	0.812421	0.704528	0.04852	-0.27726	0.04852	-0.27726
35Sn	-4.5517	-3.5395	-4.4504	3.2086	0.526463	0.870801	0.761707	0.930063	0.527589	1.793847	0.527589	1.793847
2C	-48.382	119.0312	-33.0418	121.5143	0.242857	0.695786	0.389824	0.623234	0.249552	0.926554	0.249552	0.926554
3C	85.9541	-338.234	75.4805	-325.813	0.222186	0.120747	0.508269	0.063366	0.079171	0.279923	0.079171	0.279923
						Ethanol						
1O	151.6237	272.1817	132.808	261.4736	0.130365	0.179243	0.748562	0.062492	-0.1939	-0.76773	-0.1939	-0.76773
5N	136.197	-142.031	-123.666	-140.868	0.745975	0.865021	0.56683	0.499491	-0.37359	-0.96555	-0.37359	-0.96555
23O	592.01	496.286	456.6419	427.1608	0.442882	0.39728	0.263612	0.468624	-0.23426	-0.54458	-0.23426	-0.54458

Table 2. Contd.

24O	37.5154	-127.326	-34.9162	-148.035	0.753587	0.681847	0.134379	0.53522	-0.33361	-0.87974	-0.33361	-0.87974
27S	202.7531	124.6111	-150.798	-136.098	0.295062	0.992988	0.815267	0.705183	0.048393	-0.27741	0.048393	-0.27741
35Sn	-4.5531	-3.5293	-4.4522	3.2027	0.525598	0.872496	0.761017	0.929497	0.527108	1.793564	0.527108	1.793564
2C	-48.4346	119.2185	-33.0688	121.6555	0.248657	0.690011	0.396788	0.615337	0.249455	0.926916	0.249455	0.926916
3C	85.8151	-335.378	75.3244	-323.209	0.217786	0.114918	0.51115	0.057308	0.079446	0.278123	0.079446	0.278123

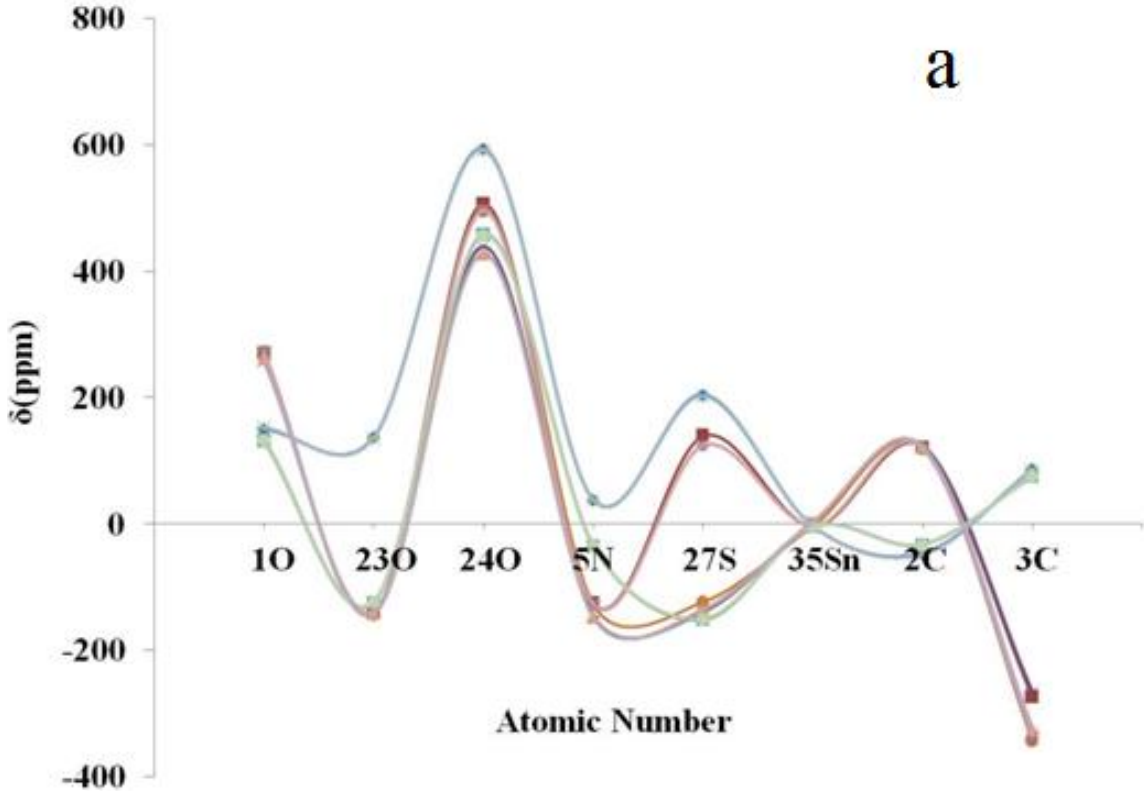

Figure 3. Graphs of the δ(ppm) versus atomic number (a), η versus atomic number (b), total atomic charge (a.u) versus atomic number (c), for selected atoms of $Sn(C_6H_5)_2$(N-acetyl-L-cysteinato-O,S) – CNT complex in both gas phase and in solution obtain from the GIAO and CSGT methods.

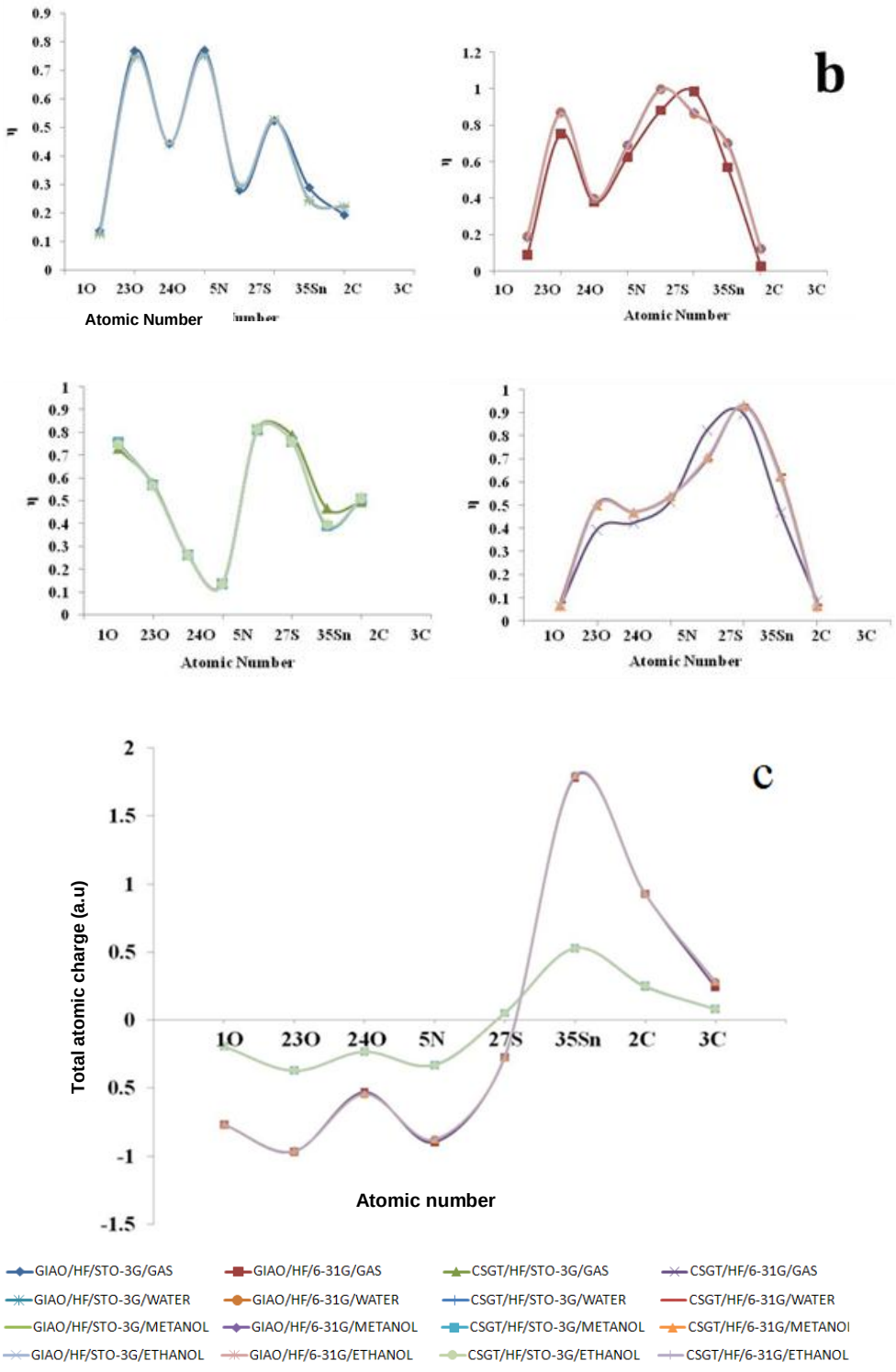

Figure 3. Contd.

Table 3. Calculated free Gibbs energies (kcal/mol) and entropies (kcal/molK) in both gas phase and in solution, for $Sn(C_6H_5)_2$(N-acetyl-L-cysteinato-O,S) – CNT complex obtained at the level of HF/ (LanL2DZ+STO-3G).

Temperature (K)	Gas phase	Water ΔG(Kcal/mol)	Ethanol	Methanol
298.15	-1764193.05971898	-1764193.1099191	-1764191.510418	-1764193.14443167
300.15	-1764193.59748769	-1764193.64894281	-1764192.03438168	-1764193.68345539
302.15	-1764194.13776641	-1764194.19047652	-1764192.56148286	-1764194.2249891
304.15	-1764194.67992762	-1764194.73452025	-1764193.09046655	-1764194.76903282
306.15	-1764195.22522635	-1764195.28107397	-1764193.62133275	-1764195.31558655
308.15	-1764195.77240758	-1764195.82951021	-1764194.15533645	-1764195.86402278
310.15	-1764196.32147131	-1764196.38045645	-1764194.69122265	-1764196.41496902
312.15	-1764196.87367255	-1764196.93328519	-1764195.22899136	-1764196.96842527
313.15	-1764197.15040068	-1764197.21064081	-1764195.49944447	-1764197.24578089
298.15	0.268331	0.269013	0.261607	0.269043
300.15	0.2695	0.270183	0.262764	0.270213
302.15	0.270668	0.271352	0.263919	0.271382
304.15	0.271834	0.272519	0.265074	0.272549
306.15	0.272999	0.273685	0.266227	0.273715
308.15	0.274163	0.27485	0.267378	0.274879
310.15	0.275326	0.276013	0.268529	0.276043
312.15	0.276487	0.277176	0.269678	0.277205
313.15	0.277068	0.277756	0.270253	0.277785

values than the C-3 nucleus (Figure 3b). Since the electrostatic properties are mainly dependent on the electronic densities at the sites of nuclei, Oxygen plays a significantly different role among the other nuclei (S, C, Sn and N atoms). Total atomic charge for O-23 nucleus is minimum meaning O-23 nucleus has maximum electron shielding (Figure 3c). This leads to a minimum chemical shift tensor (δ) at the site of O-23 atom (Figure 3a). Also, Figure 3b shows that O-23 has large amounts of η in both gas phase and solution. The results in Figure 3a indicate that, the calculated chemical shift tensor at the site of O-23 is reduced by increasing dielectric constant (ε) of solvent. Also, with increase of dielectric constant from gas phase to water, the asymmetry parameter value at the site of O-23 atom increases. In this regard, it seems that the NMR parameters at the site of O-23 are significantly influenced by intermolecular hydrogen- bonding interactions. On the other hand, Figure 3c shows that O-23 posses more negative than O-24 nucleus. This difference in the total atomic charge values lead to a maximum chemical shift tensor (δ) at the site of O-24 atom (Figure 3a). As shown in Figure 3c, O-24 has maximum asymmetry parameter in water, but the quantity in Methanol is minimum. Furthermore, the chemical shift tensor (δ) at the site of O-24 decreases in the order Gas Phase > Ethanol > Methanol > Water (Figure 3a). It can be said that NMR parameters at the site of O-24 nucleus are significantly influenced by intermolecular hydrogen- bonding interactions. Moreover, the chemical shift tensor (δ) at the site of O-1 decreases in the order Water > Ethanol > Methanol > Gas Phase (Figure 3a). The observed effect is probably due to the intermolecular hydrogen- bonding interactions at the site of O-1 nucleus. Finally, the chemical shift tensor (δ) at the site of Oxygen decreases in the order O-24 > O-1 > O-23. It can be said that O-23 has maximum electron shielding but the quantity in the

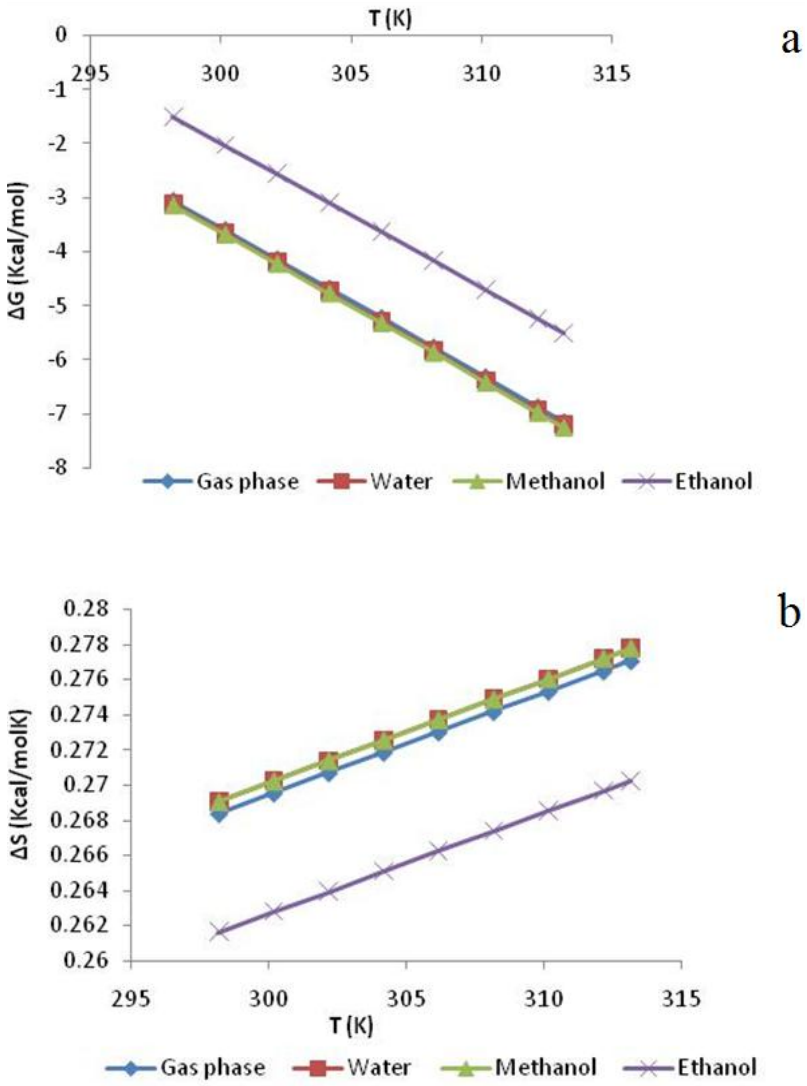

Figure 4. Plots of the ΔG (Kcal/mol) versus the T (K) (d) and ΔS (Kcal/molK) versus the T (K) (c) for $Sn(C_6H_5)_2$(N-acetyl-L-cysteinato-O,S) – CNT Complex in both gas phase and in solution, obtain from the (LanL2DZ+STO-3G) calculations.

O-24 nuclei is minimum.

Thermodynamic analysis

The computed free Gibbs energies (ΔG) and entropy changes (ΔS) in both gas phase and in solution, for $Sn(C_6H_5)_2$(N-acetyl-L-cysteinato-O,S) – CNT complex at the different temperature are given in Table 3. Based on these results, the plots of calculated free Gibbs energies (ΔG) and entropies (ΔS) versus the physiological temperature are displayed in Figures 4a and b respectively. As shown in Table 3 and Figure 4 it can be said $Sn(C_6H_5)_2$(N-acetyl-L-cysteinato-O,S) – CNT complex has negative values of free Gibbs energies (ΔG) in both gas phase and in solution. Also, the calculated entropies (ΔS) for $Sn(C_6H_5)_2$(N-acetyl-L-cysteinato-O,S) – CNT system have positive values (Table 3 and Figure 4c). These results can be related to the structural stability of the $Sn(C_6H_5)_2$(N-acetyl-L-cysteinato-O,S) – CNT in both gas phase and in solution.

The results in Figure 4 show that, the calculatedfree Gibbs energies (ΔG) of $Sn(C_6H_5)_2$(N-acetyl-L-cysteinato-O,S) – CNT system decrease in the order Ethanole > Gas phase > Water > Methanol. These results indicate that $Sn(C_6H_5)_2$(N-acetyl-L-cysteinato-O,S) – CNT has maximum stability in Methanol at 313K. And also, the calculated entropies (ΔS) decrease in the order Methanol > Water > Gas phase > Ethanol. It can be said that $Sn(C_6H_5)_2$(N-acetyl-L-cysteinato-O,S) – CNT has maxi

mum entropies (ΔS) in Methanol but the quantity in Ethanol is minimum.

Conclusion

1. As the dielectric constant of the solvent increases, the dipole moment (μ) of $Sn(C_6H_5)_2$(N-acetyl-L-cysteinato-O,S) – CNT increased.
2. The calculated chemical shift tensor (δ) at the site of Oxygen decreases in the order O-24 > O-1 > O-23.
3. O-23 has minimum total atomic charge but the quantity in the Sn-35 nucleus is maximum.
4. The NMR parameters (δ, η) at the site of S-27 is influenced by nonspecific solute-solvent interaction such as polarisability/polarity but the quantity at the sites of nitrogen and oxygen as are significantly influenced by intermolecular hydrogen- bonding interactions.
5. The thermodynamic analysis show that $Sn(C_6H_5)_2$(N-acetyl-L-cysteinato-O,S) – CNT has maximum stability in Methanol at 313K.
6. Carbon nanotube that used in this study can act as a good carrier for $Sn(C_6H_5)_2$(N-acetyl-L-cysteinato-O,S) in physiological temperature.
7. Since the $Sn(C_6H_5)_2$(N-acetyl-L-cysteinato-O,S) – CNT complex has little stability in H_2O, pure water cannot act as a good solvent for drug delivery of drug-cnt system.

ACKNOWLEDGMENT

My sincere thanks to Dr. Shahram Aramideh for his critical comments on the manuscript.

REFERENCES

Banerjee S, Hemraj-Benny T, Wong SS (2005). Covalent surface chemistry of singlewalled carbon nanotubes. Adv. Mater. 17:17–29.
Bianco A, Kostarelos K, Partidos CD, Prato M (2005). Biomedical applications of functionalised carbon nanotubes. Chem. Commun. pp. 571–577.
Clarke MJ, Zhu F, Frasca DR (1999). Non-platinum chemotherapeutic metallopharmaceuticals. Chem. Rev. 99:2511–2534.
Ditchfield R (1972). Molecular-orbital theory of magnetic shielding and magnetic susceptibility. J. Chem. Phys. 56:5688–5692.
Eng G, Whalen D, Zhang YZ, Kirksey A, Otieno M, Khoo LE, James BD (1996). Appl. Organomet. Chem. 10(7):501–503.
Frisch MJ, Trucks GW, Schlegel HB, Scuseria GE, Robb MA, Cheeseman JR, Zakrzewski VG, Montgomery JA Jr, Stratmann RE, Burant JC, Dapprich S, Millam JM, Daniels AD, Kudin KN, Strain MC, Farkas O, Tomasi J, Barone V, Cossi M, Cammi R, Mennucci B, Pomelli C, Adamo C, Clifford S, Ochterski J, Petersson GA, Ayala PY, Cui Q, Morokuma K, Malick DK, Rabuck AD, Raghavachari K, Raghavachari JB, Cioslowski J, Ortiz JV, Baboul AG, Stefanov BB, Liu G, Liashenko A, Piskorz P, Komaromi I, Gomperts R, Martin RL, Fox DJ, Keith T, Al-Laham MA, Peng CY, Nanayakkara A, Gonzalez C, Challacombe M, Gill PMW, Johnson B, Chen W, Wong MW, Andres JL , Gonzalez C, Head-Gordon M, Replogle ES, Pople JA (1998). Gaussian 98 Revision A.7. Gaussian, Inc., Pittsburgh.
Gielen M (1996). Tin-Based Antitumor Drugs. Coord. Chem. Rev. 151:41–51.
Girasolo MA, Rubino S, Portanova P, Calvaruso G, Stocco G, Ruisi G (2010). Novel diorganotin(IV) derivatives of l-Arginine (HArg), Na-(tert-Butoxycarbonyl)-l. J. Organom. Chem. 695:609–618.
Goldberg DE, Sharma V, Oksman A, Gluzman I, Wellems TE, Piwnica-Worms D (1997). Probing the metal (III) coordination complexes. J. Biol. Chem. 272(10):6567–6572.
Hay PJ, Wadt WR (1985). Ab initio effective core Potentials for the transition metal atoms Sc to Hg. J. Chem. Phys. 82:270-270.
Iijima S (1991). Helical microtubules of graphitic carbon, Nature, 354:56–58.
Keith TA, Bader RFW (1993). Calculation of Magnetic Response. Chem. Phys. Lett. 210:223-223.
Klumpp C, Kostarelos K, Prato M, Bianco A (2006). Functionalized carbon nanotubes as emerging nanovectors for the delivery of therapeutics, Biochim. Biophys. Acta: Biomembr. 1758:404–412.
Kostarelos K, Lacerda L, Pastorin G (2007). Cellular uptake of functionalized carbon nanotubes is independent of functional group and cell type. Nat. Nanotechnol. 2:108–113.
K♀pf-Maier P, K♀pf H (1987). Anti-HIV Effects of Gramicidin in vitro. Chem. Rev. 87(5):1137–1152.
Miertus M, Scrocco E, Tomasi J (1981). From Theozymes to Artificial Enzymes: Enzyme-Like Receptors. Chem. Phys. 55:117–129.
Miertus S, Tomasi J (1982). Approximate evaluations of the electrostatic free energy and internal changes in solution. Chem. Phys. 65:239–252.
Mollaamin F, Layali I, Ilkhani A R, Monajjemi M (2010a). Nanomolecular simulation of the voltage–gated potassium channel protein by gyration radius study. Afr. J. Microbiol. Res. 4(24):2795-2803.
Mollaamin F, Shahani poor K, Nejadsattari T, Monajjemi M (2010b). Bio-nanomodeling of active site in oxidized azurin using by computational methods. Afr. J. Microbiol. Res. 4(20):2098-2108.
Mollaamin F, Varmaghani Z, Monajjemi M (2011). Dielectric effect on thermodynamic properties in vinblastine by DFT/Onsager modeling. Phys. Chem. Liquids 49(3):318-336.
Monajjemi M, Baie M T, Mollaamin F (2010a). Interaction between threonine and cadmium cation in [Cd(Thr)n]2+ (n = 1—3) complexes: density functional calculations. Rus. Chem. Bull. 59(5):886-889.
Monajjemi M, Lee V S, Khaleghian M, Honarparvar B, Mollaamin F (2010b). Theoretical Description of Electromagnetic Nonbonded Interactions of Radical, Cationic and Anionic NH2 BHNBHNH 2 Inside of the B 18 N18Nanoring. J. Phys. Chem. C. 114:15315-15330.
Monajjemi M. Chahkandi B (2005). Theoretical investigation of hydrogen bonding in Watson-Crick, Hoogestein and their reversed and other models: comparison and analysis for configurations of adenine-thymine base pairs in 9 models. J. Molecular Structure-Theochem. 714(1):43-60 JAN 31.
Nath M, Pokharia S, Yadav R (2001). Calix[4]arenes as Molecular Platforms in Magnetic Resonance Imagery. Coord. Chem. Rev. 215:99–149 and references therein.
Pastorin G, Wu W, Wieckowski SB, Briand J-P, Kostarelos K, Prato M, (2006). Double functionalisation of carbon nanotubes for multimodal drug delivery. Chem. Commun. pp. 1182–1184.
Pellerito L, Prinzivalli C, Casella G, Fiore T, Pellerito O, Giuliano M, Scopelliti M, Pellerito C (2010). Diorganotin(IV) N-acetyl-L-cysteinate complexes: synthesis. J. Inorg. Biochem. 104:750–758.
Pessoa JC, Covaco I, Correia I, Duarte MT, Gillard R D, Henriques RT, Higes FJ, Madeira C, Tomaz I (1999). Preparation and derived from amino acids and aromatic o-hydroxyaldehydes. Inorg. Chim. Acta, 293(1):1–11.
Plesch G, Friebel C, Svajlenova O, Kratsmar-Smogrovic J, Mlynarcik D (1988). Copper (II) complexes of the general composition Cu(ligand)2X2 (where X=Cl−, Br. Inorg. Chim. Acta 151(2):139–143.
Popov AM, Lozovik YE, Fiorito S, Yahia LH (2007). Biocompatibility and applications of carbon nanotubes in medical nanorobots. Int. J. Nanomed., 2: 361–372.
Pulay P, Wolinski K, Hinton JF (1990). The 3–21+G basis set for first row elements. J. Am. Chem. Soc. 112:8251–8260.
Raffa V, Ciofani G, Nitodas S, Karachalios T, D'Alessandro D, Masini M (2008). Can the properties of carbon nanotubes influence their internalization by living cells? Carbon 46:1600–1610.
Tzimopoulos D, Sanidas I, Varvogli AC, Czapik A, Gdaniec M, Nikolakaki E, Akrivos P D (2010). Detection of elevated antibodies

against SR. J. Inorg. Biochem. 104:423–430.
Wadt WR, Hay PJ (1985). DeMon2k. J. Chem. Phys. 82:284-284.
Wang MZ, Meng Z (2006). Determine the effects of acupuncture on specific clinical symptoms in. Acupuncture for the Prevention of Radiation-Induced Xerostomia. J. Fu, Appl. Radiat. Isot. 64(2):235–240.
Wang MZ, Meng Z, Liu B, Cai G, Zhang C, Wang X (2005). Effects of extrusion and a Magnesium Lattice. Inorg. Chem. Commun. 8(4):368–371.
Wrackmeyer B (1985). A multinuclear NMR study unambiguously confirmed that metal tetraolates retain their polynuclear structure in solution. Annu. Rep. NMR Spectrosc. 16:73–186.
Zhang X, Meng L, Lu Q, Fei Z, Dyson PJ (2009). Targeted delivery and controlled release of doxorubicin to cancer cells using modified single wall carbon nanotubes. Biomaterials 30:6041–6047.